ADVANCED MATERIALS

face consisting of {100} faces possesses three-fold axes at the apexes. The four-fold symmetry at the center of the {100} faces may not be obvious when the cubes form interfaces with the Au surface using {110} or {111} faces.

In summary, we have demonstrated a methodological approach for utilizing the preferential adsorption of amphiphiles during the electrodeposition process to precisely control the shapes of Cu_2O crystals. The pH dependence of preferential adsorption made it possible to selectively tune the growth rate of Cu_2O crystals along the <111> directions and therefore, their final morphology. The detailed nature of the preferential adsorption of SDS on the {111} Cu_2O faces and its pH-dependence are currently under investigation. The resulting electrodes will be useful to elucidate any dependence of the catalytic, electrochemical, and photoelectrochemical properties on different crystallographic planes of Cu_2O particles (e.g., {100} versus {111}).[18–22]

Experimental

Preparation of Electrodes: For the counter electrode, 100 Å of titanium followed by 500 Å of platinum were deposited on clean glass slides by sputter coating. For the working electrode, 100 Å of chromium followed by 500 Å of gold were deposited on clean glass slides by thermal evaporation. SEM images of the resulting Au electrodes showed a smooth and featureless surface (grain size < 50 nm) and the XRD measurement revealed a strong preferential orientation of Au {111} planes parallel to the substrate.

Electrodeposition of Cu_2O: Cu_2O crystals were prepared by cathodic deposition from aqueous solutions of 0.02 M $Cu(NO_3)_2 \cdot 6H_2O$. SDS (5 wt.-% = 0.17 M) or sodium sulfate (0.17 M) was introduced as additives to produce the results shown in Figures 1b,c, Figure 2, and Figure 4b. The pH of the solutions was adjusted by adding HCl and NaOH when required. The pH of the solutions containing SDS was adjusted and measured before SDS was added because the presence of SDS in the solution complicates reliable pH readings. All the crystals shown in Figures 1,2 were deposited galvanostatically (0.7 $A\,m^{-2}$) at 60 °C for 20 min without stirring except for the octahedral crystals shown in Figure 1b, which were produced by pulsed deposition composed of current pulses of 1.8 $A\,m^{-2}$ for 0.1 s followed by a resting time of 0.9 s. The net deposition time was 3 min (total deposition time was 30 min). Octahedral crystals deposited using continuous galvanostatic deposition showed less-uniform crystal sizes.

Received: February 7, 2004
Final version: March 30, 2004

[1] S. Mann, *Angew. Chem. Int. Ed.* **2000**, *39*, 3392.
[2] J. H. Adair, E. Suvaci, *Curr. Opin. Colloid Interface Sci.* **2000**, *5*, 160.
[3] Y. Sun, Y. Xia, *Science* **2002**, *298*, 2176.
[4] C. A. Orme, A. Noy, A. Wierzbicki, M. T. McBride, M. Grantham, H. H. Teng, P. M. Dove, J. J. De Yoreo, *Nature* **2001**, *411*, 775.
[5] L. Manna, E. C. Scher, A. P. Alivisatos, *J. Cluster Sci.* **2002**, *13*, 521.
[6] J. W. Mullin, *Crystallization*, Butterworths, London **1971**.
[7] H. E. Buckley, *Crystal Growth*, Wiley, New York **1951**.
[8] E. Budevski, G. Staikov, W. J. Lorenz, in *Electrochemical Phase Formation and Growth*, VCH, New York **1996**.
[9] D.-L. Lu, K.-I. Tanaka, *J. Electrochem. Soc.* **1996**, *143*, 2105.
[10] T. Yoshida, H. Minoura, *Adv. Mater.* **2000**, *12*, 1219.
[11] a) Y. C. Zhou, J. A. Switzer, *Mater. Res. Innovations* **1998**, *2*, 22. b) J. A. Switzer, H. M. Kothari, E. W. Bohannan, *J. Phys. Chem. B* **2002**, *106*, 4027.
[12] a) R. Liu, E. W. Bohannan, J. A. Switzer, F. Oba, F. Ernst, *Appl. Phys. Lett.* **2003**, *83*, 1944. b) R. Liu, F. Oba, E. W. Bohannan, F. Ernst, J. A. Switzer, *Chem. Mater.* **2003**, *15*, 4882.
[13] J. A. Switzer, C.-J. Hung, L.-Y. Huang, E. R. Switzer, D. R. Kammler, T. D. Golden, E. W. Bohannan, *J. Am. Chem. Soc.* **1998**, *120*, 3530.
[14] Z. L. Wang, *J. Phys. Chem. B* **2000**, *104*, 1153.
[15] J.-F. Liu, W. A. Ducker, *J. Phys. Chem. B* **1999**, *103*, 8558.
[16] Cu_2O crystallizes in the space group *Pn*-3*m* (S. G.# 224). For this space group (*h*00) reflections with $h \neq 2n$ are systematically absent.
[17] Below 40 °C co-deposition of Cu_2O and Cu occurs, forming Cu/Cu_2O composite films.
[18] K. H. Schulz, D. F. Cox, *J. Catal.* **1993**, *143*, 464.
[19] M. Hara, T. Kondo, M. Komoda, S. Ikeda, K. Shinohara, A. Tanaka, J. N. Kondo, K. Domen, *Chem. Commun.* **1998**, 357.
[20] a) P. E. de Jongh, D. Vanmaekelbergh, J. J. Kelly, *Chem. Mater.* **1999**, *11*, 3512. b) P. E. de Jongh, D. Vanmaekelbergh, J. J. Kelly, *Chem. Commun.* **1999**, 1069.
[21] J.-M. Zen, Y.-S. Song, H.-H. Chung, C.-T. Hsu, A. S. Kumar, *Anal. Chem.* **2002**, *74*, 6126.
[22] W. Siripala, A. Ivanovskaya, T. F. Jaramillo, S.-H. Baeck, E. W. McFarland, *Sol. Energy Mater. Sol. Cells* **2003**, *77*, 229.

Large Spectral Birefringence in Photoaddressable Polymer Films**

By *Beth L. Lachut*, *Stefan A. Maier*, *Harry A. Atwater*,* *Michiel J. A. de Dood*, *Albert Polman*, *Rainer Hagen*, and *Sergej Kostromine*

Polymers containing azobenzene side-chains have attracted much attention due to their high optical activity upon exposure to polarized electrical and optical fields. Initially isotropic films develop extremely large in-plane birefringences $\Delta n = n_\perp - n_\parallel$ (where $n_\perp$ and $n_\parallel$ are the refractive indices in the direction perpendicular and parallel to the writing polarization, respectively) when exposed to normally incident polar-

[*] Dr. H. A. Atwater, B. L. Lachut, Dr. S. A. Maier[+]
Thomas J. Watson Laboratory of Applied Physics
California Institute of Technology
Pasadena, CA 91125 (USA)
E-mail: haa@caltech.edu
Dr. M. J. A. de Dood, Dr. A. Polman
FOM Institute of Atomic and Molecular Physics
Kruislaan 407, NL-1098 SJ Amsterdam (The Netherlands)
Dr. R. Hagen, Dr. S. Kostromine
Bayer Polymers
D-51368 Leverkusen (Germany)
[+] Present address: Dept. of Physics, University of Bath, Bath BA2 7AY, UK.

[**] Pieter Kik is gratefully acknowledged for stimulating discussions, and Hans Mertens for his help with transmission measurements. The work at Caltech was supported by the Air Force Office of Scientific Research and work at AMOLF is part of the research program of FOM, which is financially supported by NWO.

  DOI: 10.1002/adma.200400121

ized light at wavelengths within the absorption band (typically 300–630 nm). Previous work has shown that large optical birefringences up to 0.36 at 780 nm are possible and that the induced birefringence can be written and unwritten thousands of times.[1,2] After inducing birefringence into the film, illumination by unpolarized or perpendicularly polarized light within the absorption band drives the film back to its isotropic state. Such rewritable birefringent materials are important for many applications, including optoelectronic devices, planar waveguides, alignment layers for polarized light-emitting diodes, and optical data storage.[3–5]

At the molecular level, the formation of optical birefringence can be explained with the angular hole-burning model.[1] Azobenzene side chains attached to the poly(methyl methacrylate) (PMMA) polymer backbone undergo photoisomerization cycles between their *trans*- and *cis*-isomer states upon illumination with polarized light until the long axes of the chromophores are oriented perpendicular to the electric field. In this orientation, the side chain cannot be further addressed by the polarized field. Once excited to the *cis*-state, the azobenzene may photochemically or thermally relax and reorient via rotational diffusion. In general, photoinduced birefringence for these polymers is stable for long times and can be read non-destructively by illumination at wavelengths outside the absorbing region.

We report on an azobenzene-functionalized homopolymer that has been engineered to maximize birefringence. It shows an extremely large spectral birefringence $\Delta n(\omega)$ throughout the entire measured spectral range of 630 to 1700 nm. This polymer has densely packed side chains comprising two azobenzene units. The observed generation of large Δn upon optical excitation with polarized light described below is believed to be due to a relatively large flexibility in movement of these units due to cooperative rearrangements. An in-situ study of the effect of writing intensity on room-temperature birefringence growth has been performed, and polarization-dependent transmission spectroscopy has been used to characterize the birefringence. Insight into the mechanism for the decrease in maximum Δn after the first rewrite cycle is gathered from a comparative analysis of Δn and photobleaching with writing time. A decrease in absorption of the writing source is assumed to be indicative of photobleaching, which is discussed below.

The polymer under investigation consists of a PMMA backbone with a single chromophore unit (see Fig. 1), which produces and stabilizes the birefringence.[6] The molecular-number average and weight average for this polymer are $M_n = 5.55 \times 10^3$ g mol^{-1} and $M_w = 1.15 \times 10^4$ g mol^{-1}, respectively, as measured by fast gel-permeation chromatography using a PMMA calibration. We used the Mark–Houwink relationship with parameters $K = 0.1086$ and $a = 0.3775$, which is valid for determining molecular weights for this type of photoaddressable polymer. The residual amount of monomer present is estimated to be less than 1 %. Small levels of impurities from oil pumps or the substrate surface may be present, but have no effect on the photo-orientation process. Thin photo-

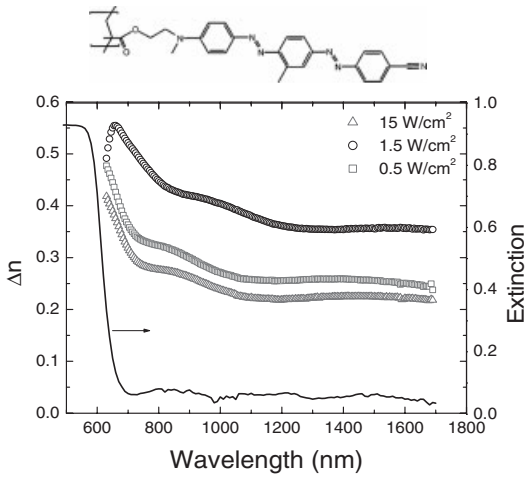

Figure 1. Steady-state spectral birefringence for a 490 nm thick PAP film, whose exposure characteristics are described in Figure 3, measured via polarized transmission spectroscopy following an exposure dose of 1 J cm^{-2}. A writing intensity of 1.5 W cm^{-2} generates the largest spectral birefringence, with a peak of 0.56 at 660 nm and continued high birefringence out to 1500 nm ($\Delta n = 0.36$). Also shown is the extinction spectrum of an unwritten PAP film on a glass substrate obtained via transmission measurements. The composition of the azobenzene chromophore is shown above.

addressable polymer (PAP) films were obtained by dissolving the PAP in tetrahydrofuran (99.9 % pure from Aldrich Corp.) at concentrations of 25–100 g L^{-1} and then spin-coating it onto clean glass slides at 4000 rpm. The films were dried for 1 h at 60 °C (glass transition $T_g = 95$ °C). Homogenous films of 150–600 nm thickness with a surface roughness of 1–2 nm were obtained as determined by an Alpha-Step profilometer and atomic force microscope.

Figure 1 shows the extinction spectrum of a thin polymer film calculated from transmission and reflectance data obtained via spectroscopic ellipsometry (Woollam VASE). Note the steep drop in the extinction curve around 630 nm (right axis). As scattering due to film surface fluctuations can be safely neglected in the experimental wavelength range, given the measured roughness of 1–2 nm, the measured extinction effectively is a measurement of polymer absorption. Reflection losses of approximately 10 % resulting from the air/polymer interface account for the non-perfect transmission above 630 nm.

The initially optically isotropic polymer film was exposed to a polarized argon laser beam at $\lambda = 488$ nm, and thus written at a wavelength well within the polymer absorption band. The optical anisotropy of the PAP film was measured at discrete wavelengths using either a 632.8 nm HeNe laser or a 670 nm diode laser. The polarization direction of the read beam was offset by 45° with respect to the writing beam, and the amount of birefringence was quantified using a standard method discussed elsewhere.[7] In order to achieve uniform writing over a well-defined area, a 4 mm wide aperture was placed in the Ar laser beam path after expansion through a concave lens ($f = -25$ mm). After passing through the sample, the writ-

ADVANCED MATERIALS

ing beam was blocked in the detection pathway by a 550 nm long pass color filter. A polarized beam splitter split the read laser into two components, one with polarization parallel to the initial polarization $I_{\parallel}$, and one with polarization perpendicular to the initial polarization $I_{\perp}$. Germanium photodetectors were used to monitor the intensity of the He–Ne beams. The induced uniaxial birefringence was determined from the rotation in polarization state of the reading source via

$$\Delta n = \frac{\lambda}{\pi d}\sin^{-1}\sqrt{\frac{I_{\perp}}{I_{\perp}+I_{\parallel}}} \quad (1)$$

where λ is the probe wavelength, and d is the film thickness.

Figure 2 shows birefringence as a function of laser dose for a $\lambda = 488$ nm write source (intensity of 121 mW cm^{-2}) on film

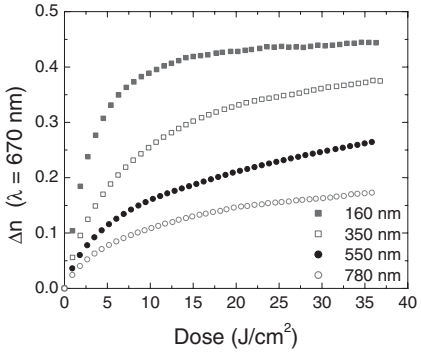

Figure 2. Birefringence of films of 160, 350, 550, and 780 nm thickness as read by a 670 nm diode laser for a writing intensity of 121 mW cm^{-2} at 488 nm.

thicknesses ranging from 160–780 nm. Birefringence was read at 670 nm, and for clarity every fifth data point is plotted. The saturation dose is largely determined by film thickness, as 90 % of peak birefringence is reached at approximately 11 J cm^{-2} for 160 nm films and 370 J cm^{-2} for 550 nm films. This indicates that the PAP material exhibits high extinction and is optically "thick" and thus written inhomogeneously throughout its thickness for films thicker than 500 nm. We thus conclude that for maximum speed and efficiency it is best to use optically thin polymer films in the range of 100–150 nm.

Although the polymer side chains are relatively bulky compared to azobenzene-side-chain polymers previously discussed in the literature,[8] large birefringences can be achieved due to the cooperative motion of the densely packed side groups. The data in Figure 2 can be fit by a biexponential of the form:

$$\Delta n(t) = \Delta n_{\text{slow}}(1 - e^{-k_{\text{slow}}t}) + \Delta n_{\text{fast}}(1 - e^{-k_{\text{fast}}t}) \quad (2)$$

where Δn_{slow} and Δn_{fast} are saturation values of the slow and fast terms, respectively; k_{slow} and k_{fast} are the corresponding growth constants; and t is the writing time.[1–2] We suggest that the fast growth mechanism describes the reorientation of the side groups initially accessible to the optical field. Since the polymer is highly absorbing at the write wavelength of 488 nm ($\alpha_{\text{initial}} \simeq 16\ \mu\text{m}^{-1}$, where α is the absorption coefficient), there is a dramatic fall-off in the intensity within the film thickness (1/e decay length $\simeq$ 62 nm). Therefore, the slower growth component may result from in-situ bleaching. Specifically, chromophores that are reoriented perpendicular to the substrate due to angular hole burning show a quenched absorption, which enables the excitation light to orient chromophores lying further away from the film surface ($\alpha_{\text{final}} \simeq 7\ \mu\text{m}^{-1}$). The majority of the bleaching is believed to be from angular hole burning; however, some destructive processes may be present as well. Maximum birefringence occurs when the contribution to the total Δn is dominated by Δn_{fast} and k_{slow}/I is minimal (I is the writing intensity). Therefore, we look to optimize writing intensity and film thickness such that $\Delta n_{\text{fast}}/\Delta n$ is maximized and k_{slow} is as small as possible.

Figure 3 shows birefringence growth curves (read at 633 nm) as a function of laser dose for a $\lambda = 488$ nm writing

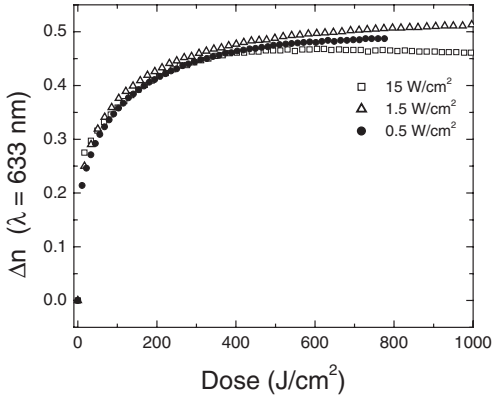

Figure 3. Photoinduced birefringence as a function of dose for a 488 nm Ar^+ ion writing laser. 512 nm thick films were written at intensities of 0.5 W cm^{-2}, 1.5 W cm^{-2}, and 15 W cm^{-2} and read in situ by a 633 nm HeNe laser. Writing intensity appears to negligibly affect the peak birefringence at 633 nm.

source with intensities of 0.5 W cm^{-2}, 1.5 W cm^{-2}, and 15 W cm^{-2} on a 512 nm thick PAP sample (for clarity every twentieth and tenth data point were plotted for 0.5 W cm^{-2} and 1.5 W cm^{-2}, respectively). The birefringence of the initially isotropic film shows an initial rapid increase followed by a gradual increase to a saturation value of approximately $\Delta n = 0.5$ for doses near 1000 J cm^{-2}. This large saturation dose is a consequence of using an optically thick polymer film, and the saturation can be reduced when thinner films are employed. In all cases, very large birefringences at 633 nm are obtained: $\Delta n = 0.51$ at 1.5 W cm^{-2}, $\Delta n = 0.49$ at 0.5 W cm^{-2}, and $\Delta n = 0.46$ at 15 W cm^{-2}. Considering the thirty-fold difference in writing intensity and only 10 % variation in final Δn, we thus conclude that writing intensity appears to have a small effect on birefringence at 633 nm. Lack of strong inten-

sity dependence on peak birefringence at 633 nm suggests that a photochemical rather than thermal process dominates writing. Therefore, in a confocal microscopy setup where a typical writing intensity might be 1 mW with a spot size of 1 μm diameter, the writing time for a 160 nm thick film to reach 90 % of peak birefringence would be less than 100 μs.

In addition to the in-situ birefringence measurements at 633 nm in Figure 3, it is also desirable to characterize the spectral Δn over an extended wavelength range farther away from the absorption band, including the technologically important telecommunications band (1300–1500 nm). For this purpose, polarization-dependent transmission measurements were performed using a spectroscopic ellipsometer (Woollam VASE), and results are shown in Figure 1 for intensities of 0.5 W cm^{-2}, 1.5 W cm^{-2}, and 15 W cm^{-2} (left axis). The writing scenarios were similar to that described in Figure 3, where the fluences for each writing intensity were approximately equal to 1000 J cm^{-2}. Data was collected over the wavelength range 630–1700 nm, and the data at 633 nm is consistent with that observed in Figure 2. The birefringence remains high over the entire wavelength range as expected for off-resonance excitation near the molecular natural frequency of vibration. The writing intensity of 1.5 W cm^{-2} showed largest birefringence over the entire spectral range, with a maximum at 660 nm ($\Delta n = 0.56$) and continued high Δn out to 1700 nm ($\Delta n = 0.36$).

Although at 633 nm Δn is not largely affected by writing intensity for a fixed dose, the birefringence spectra differ at longer wavelengths for various write intensities. For example, at 1500 nm Δn for 0.5 W cm^{-2} and 1.5 W cm^{-2} differ by 0.10. The disparity must be due to different writing kinetics influenced by writing intensity, an effect that must be further studied.

As mentioned earlier, polymer rewritability is important for optical data storage and waveguide tuning applications. In order to characterize the rewritability of the PAP film, photobleaching and birefringence of a 490 nm thick PAP sample were monitored in a Zeiss Axiovert inverted optical microscope. A halogen lamp with a linear polarizer was used as the writing source with an intensity of 41 mW cm^{-2}. The lamp spectrum is shown as an inset to Figure 4. The same lamp, with its spectrum narrowed down to 665–700 nm using a long-pass filter and a 1.0 neutral density filter (hatched area in inset of Fig. 4), was used as a reading source. Measurements were taken approximately 20 s after writing to insure a reading of the steady-state film properties.

Birefringence as a function of optical exposure is shown in Figure 4, where the open squares show a rapid increase in Δn followed by saturation at ~ 185 J cm^{-2}. Also shown is the absorption of the film at 500 nm relative to the initial absorption of the unwritten film. As can be seen, $\Delta\alpha$ decreases at a similar rate to the birefringence growth. We attribute this decrease in absorption to photobleaching of the PAP film.

After the initial write cycle (at 185 J cm^{-2} in Fig. 4), the polarization was rotated by 90° and a new initial transmitted intensity I_o was measured. I_o in this orientation was 25 % lower than in the initially isotropic film, since the first write cycle

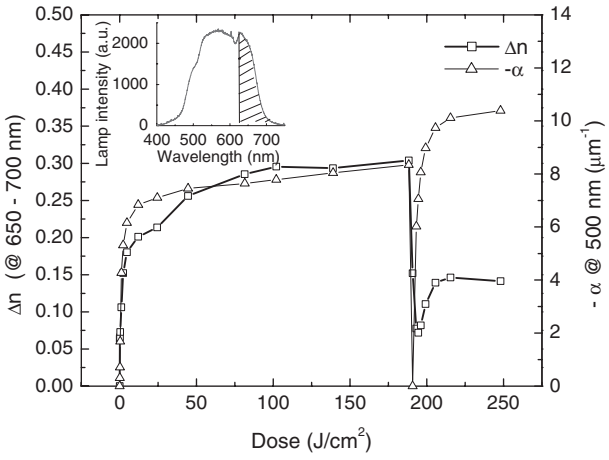

Figure 4. Birefringence and absorbance of a 490 nm thick PAP sample monitored in an inverted optical microscope. A halogen lamp with a linear polarizer was used as writing source (fluence = 41 mW cm^{-2}) and reading source (see inset for filtered lamp spectrum indicated by hatched region). At 4600 s the writing polarization was rotated 90° and birefringence and absorbance were again measured. During the second write cycle it is apparent that the decrease in saturation birefringence is a result of photobleaching, where doubled transmission of the writing source through the sample has halved the peak Δn. Plot lines are drawn to guide the eye.

oriented a large fraction of the side chains parallel to this direction, thus resulting in greater initial absorption. Film exposure was then continued. The Δn from this second write cycle saturates at 0.15, a value much lower than the first cycle. Also, the relative absorption of the film is even less (–10.4 μm^{-1}) than after the first write cycle (–8.3 μm^{-1}). The fraction $(I - I_o)/I_o$ (I_o being the initial transmitted intensity and I the transmitted intensity during writing) of transmitted 500 nm light essentially doubles from the first write cycle to the second. This suggests that the mechanism destroying the ability of the side chains to reorient and induce birefringence during the second cycle is due to photobleaching.

Photobleaching can be visually observed by the decrease in brightness of the red polymer after writing. The faster kinetics of absorption loss as compared to birefringence growth indicates that other processes in addition to chromophore orientation (angular hole burning) are contributing to a loss in absorption. Destructive contributions to photobleaching are believed to include dimer formation and side-chain orientation in the out-of-plane direction. Dimer formation results from agglomeration of the azobenzene chromophores due to dipole–dipole interactions. This effect can be undone via thermal treatment, which can be seen visually as an increase in the red color at the writing spot. However, orientation of side chains in the out-of-plane direction makes them insensitive to further excitation and is therefore not reversible by optical methods.

In conclusion, a new azobenzene-side-chain polymer that can be processed in thin-film form is shown to exhibit very large spectral birefringence from 630–1700 nm. A writing intensity of 1.5 W cm^{-2} produces maximal birefringence due to

ADVANCED MATERIALS

enhancement of polymer-side-chain mobility at room temperature, and the saturation dose is largely dependent on film thickness. We also show that polymer rewriteability is directly correlated to the degree of photobleaching that occurs during writing. The very large birefringence and high optical transparency in the 650–1600 nm wavelength range is quite promising for integrated photonic device applications of photoaddressable polymer thin films.

Experimental

Sample Preparation: Amorphous isotropic polymer films with thicknesses ranging from 160–780 nm were prepared by spinning PAP solutions in tetrahydrofuran on glass substrates. The sample thickness was determined with an Alpha-Step surface profiler, while the refractive index was measured with a spectroscopic ellipsometer.

Optical Characterization: Film birefringence was quantified in situ using a standard experimental setup [7] where the reading source (633 nm HeNe or 670 nm diode) was polarized 45° with respect to the write source (488 nm line of the Ar^+ beam). Both beams are directed onto the sample surface in normal incidence (write diameter ~1.4 mm, read diameter ~0.5 mm), and subsequently pass through polarized beam splitters. The write beam and the perpendicular-polarized component of the read beam are then directed to germanium photodetectors to obtain intensity data for the calculation of photobleaching and birefringence, respectively.

Received: January 26, 2004
Final version: April 8, 2004

[1] Y. Sabi, M. Yamamoto, H. Watanabe, T. Bieringer, D. Haarer, R. Hagen, S. Kostromine, H. Berneth, *Jpn. J. Appl. Phys., Part 1* **2001**, *40*, 1613.
[2] S. J. Zilker, T. Bieringer, D. Haarer, R. S. Stein, J. W. Van Egmond, S. Kostromine, *Adv. Mater.* **1998**, *10*, 855.
[3] E. Kim, G. Whiteside, L. K. Lee, S. P. Smith, M. Prentiss, *Adv. Magn. Opt. Reson.* **1996**, *8*, 139.
[4] X. Yang, D. Neher, S. Lucht, H. Nothofer, R. Guentner, U. Scherf, R. Hagen, S. Kostromine, *Appl. Phys. Lett.* **2002**, *81*, 2319.
[5] R. Hagen, T. Bieringer, *Adv. Mater.* **2001**, *13*, 1805.
[6] H. Korneev, O. Ramirez, R. P. Bertram, N. Benter, E. Soergel, K. Buse, R. Hagen, S. Kostromine. *J. Appl. Phys.* **2002**, *92*, 1500.
[7] N. C. R. Holme, P. S. Ramanujam, S. Hvilsted, *Appl. Opt.* **1996**, *35*, 4622.
[8] A. Natansohn, P. Rochon, *Chem. Rev.* **2002**, *102*, 4139.

Strongly Enhanced Thermal Stability of Crystalline Organic Thin Films Induced by Aluminum Oxide Capping Layers**

By *Stefan Sellner*, *Alexander Gerlach*, *Frank Schreiber*,* *Marion Kelsch*, *Nikolai Kasper*, *Helmut Dosch*, *Stephan Meyer*, *Jens Pflaum*, *Matthias Fischer*, and *Bruno Gompf*

Organic electronics is considered to be one of the key areas of future thin-film device technology. Several device applications have already been shown to exhibit convincing performance, organic light-emitting diodes being one of the most successful examples.[1–3] However, besides the obvious performance requirements, the devices have to meet stability standards, which in some cases are actually the limiting factor of technological progress.[4] Indeed, stability at elevated temperatures, high electrical-field gradients, and against exposure to corrosive gases like oxygen is crucial for many commercial applications.

It has turned out that the thermal stability of thin organic films is not only related to technical details of the fabrication procedures, but constitutes rather fundamental challenges.[5] It is thus a prerequisite to understand and to control:[6]

- interdiffusion at organic/metal interfaces during and after growth.
- thermally induced de-wetting effects at organic/inorganic interfaces.
- structural phase transformations of the organic material at temperatures often not far from temperatures of operation.
- the vapor pressure of low-weight organics at elevated temperatures.

[*] Dr. F. Schreiber, Dr. A. Gerlach
Physical and Theoretical Chemistry Laboratory, Oxford University
South Parks Road, OX1 3QZ (UK)
E-mail: frank.schreiber@chem.ox.ac.uk
S. Sellner,[+] M. Kelsch, Dr. N. Kasper,[++] Prof. H. Dosch[+]
Max-Planck-Institut für Metallforschung
Heisenbergstr. 3, 70569 Stuttgart (Germany)
S. Meyer, Dr. J. Pflaum
III. Physikalisches Institut, Universität Stuttgart
Pfaffenwaldring 57, D-70550 Stuttgart (Germany)
M. Fischer, Dr. B. Gompf
I. Physikalisches Institut, Universität Stuttgart
Pfaffenwaldring 57, D-70550 Stuttgart (Germany)
[+] Second address: Institut für Theoretische und Angewandte Physik, Universität Stuttgart, Pfaffenwaldring 57, D-70550 Stuttgart, Germany.
[++] Second address: ANKA, FZ Karlsruhe, Hermann-von-Helmholtz-Platz 1, D-76344 Eggenstein-Leopoldshafen, Germany.

[**] We acknowledge support by the Deutsche Forschungsgemeinschaft (DFG) within the Focus Program on organic field effect transistors and by the Engineering and Physical Sciences Research Council (EPSRC). We are grateful to the FZ Karlsruhe and the ANKA management for their generous support.

  DOI: 10.1002/adma.200400461